In Situ Stark Effects with Inverted Bipolar Peaks for Adsorbed CO on Pt Electrodes in 50 °C Direct Methanol Fuel Cells

Aili Bo, Sophia Sanicharane, Bhaskar Sompalli, Qinbai Fan, Bogdan Gurau, Renxuan Liu, and E. S. Smotkin*

Center for Electrochemical Science and Engineering, Illinois Institute of Technology, Chicago, Illinois 60616

Received: January 17, 2000; In Final Form: May 9, 2000

Adsorbed CO Stark tuning rates have been studied for the first time in direct methanol fuel cells on Pt black catalysts supported only on the polymer electrolyte (Nafion) in membrane electrode assemblies. The bipolar peaks resulting from the Stark shift of CO absorbance peaks are inverted, indicating an anomalous increase in the reflectivity where CO infrared absorption occurs. The vibrational Stark tuning data suggests that CO oxidation occurs on the perimeter of CO_{ads} islands, which is consistent with the formation of CO within and above Pt double layer potentials as reported by Kunimatsu. This is expected since methanol is continuously delivered to the anode at all potentials in direct methanol fuel cells.

Introduction

Direct methanol fuel cells (DMFCs) oxidize methanol directly at the anode, obviating the need for a fuel processor, thus reducing system size and complexity in comparison to reformate/air fuel cells. Tremendous advances in recent years suggest that DMFCs may compete with reformate/air fuel cells if the performances can be improved by a factor of 2.5.[1] We focus on DMFCs operating at ambient pressure and 60 °C for portable power systems. Figure 1 (comparing a quaternary PtRuOsIr catalyst developed in our lab[2,3] to a Johnson Matthey PtRu catalyst) shows typical performance curves for DMFCs operating at 60 °C with 0 gauge pressure at both the anode and at the air cathode (Pt black) obtained in our laboratory. At 0.4 V we obtain 0.1 W/cm^2. DMFC commercialization awaits further compositional improvements in the anode catalyst along with optimization of the morphology of active catalysts (i.e., the PtRuOsIr catalyst of Figure 1 has half the surface area per mass of catalysts as does the PtRu), and the development of proton conductive membranes that are impermeable to methanol.[4]

This work is a continuation of our development of in situ fuel cell catalyst characterization methods. We introduced in situ Fourier transform specular reflectance spectroscopy of catalytic surfaces of membrane electrode assemblies in working fuel cells.[5,6] The advantage of in situ methods for fuel cell studies is the avoidance of supporting electrolytes such as sulfuric acid, which introduce artifacts due to anion adsorption. In situ methods permit the study of catalytic surfaces at the three-phase interface of real fuel cell electrode systems, which consists of the metal catalyst, the polymer electrolyte (i.e., Nafion) and reactant gas streams. Our recent report of the enhancement of methanol oxidation kinetics by Nafion[7] gives credence to the necessity of in situ catalyst characterization methods for fuel cell catalysts.

The potential dependence of adsorbed CO (CO_{ads}) stretching frequencies and bandwidths, and the dependence of band position and bandwidths on the MeOH/D_2O mole ratio on high surface area fuel cell anode catalysts are examined. We demonstrate for the first time, anomalous IR bipolar peaks of CO adsorbed on fuel cell grade platinum black supported on a proton conducting polymer electrolyte Nafion film. Shi-Gang Sun et al. reported in situ abnormal IR effects with adsorbed CO on metals supported on electronically conductive polymers.[8] There have been previous reports of abnormal bipolar bands in studies of CO adsorbed on highly dispersed metals (e.g., Pt or Ir) in contact with substrates such as graphite, glassy carbon and smooth Pt surfaces.[9−12] In addition to abnormal IR effects, we examine the Stark tuning rates of CO adsorbed on highly dispersed Nafion encased catalysts, as a function of methanol concentration.

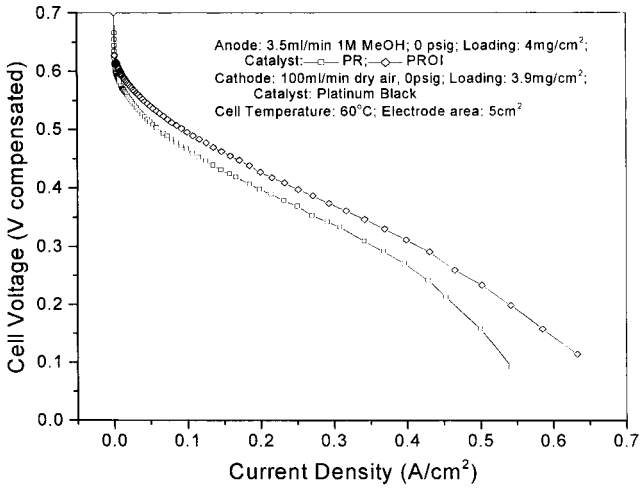

Figure 1. DMFC performance curves of commercial $Pt_{50}Ru_{50}$ vs IIT PtRuOsIr anode catalysts.

Experimental Section

FTIR Spectroscopy. Spectra of the fuel cell electrode surface were collected with a Mattson Infinity Series FTIR spectrometer with liquid nitrogen-cooled MCT detector over a spectral range of 1000−4000 cm^{-1}. The setup for in situ surface reflective FTIR spectroscopy of fuel cell membrane electrode assembly catalyst surfaces in an operating DMFC has been previously described and is shown in Figure 2.[5,6] Although a diffuse-reflection attachment is used in this study as well as in our previous studies of catalysts incorporated into membrane

10.1021/jp000222j CCC: $19.00
Published on Web 07/11/2000

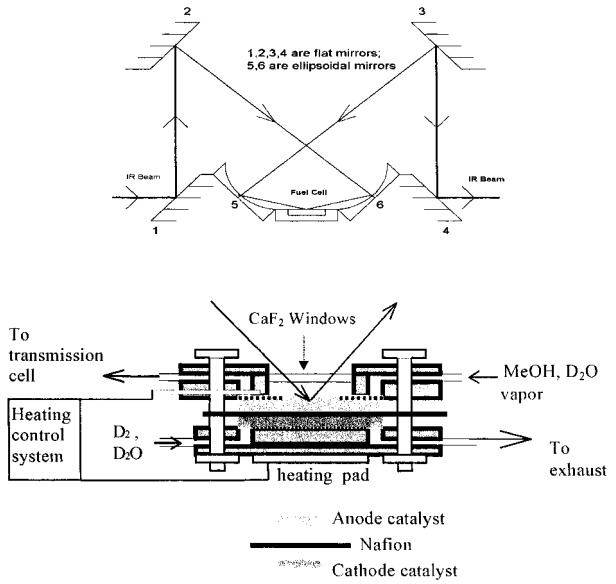

Figure 2. FTIR reflection spectroscopy and direct methanol fuel cell for FTIR spectroscopy.

electrode assemblies, Gutierrez states that when a surface consists of crystallites with radii less than $^1/_{20}$th that of the wavelength of the IR radiation, the surface can be considered as a specularly reflecting surface.[10] In this study the platinum black particle diameters (Johnson Matthey) are between 2 and 3 nm while the CO stretching wavelength is about 5 μm. Thus, the diffuse radiation can be ignored in this experiment and the integrating sphere collects essentially only the reflection beam. The data are represented as SNIFTIR spectra[13] $\Delta R/R = (R_{\text{sample}} - R_{\text{reference}})/R_{\text{reference}}$. The reference spectrum, $R_{\text{reference,}}$ was obtained at 0 V vs RHE with methanol/water vapor delivered to the anode chamber. The signal was averaged from 512 scans at a resolution of 4 cm^{-1}.

Fuel Cell Assembly. The membrane electrode assemblies (MEAs) were prepared by the decal transfer method of Wilson.[14] Nafion 117(from DuPont) was hot pressed between unsupported Pt black from (Johnson Matthey Co.) catalytic layers serving as the fuel cell anode and cathode. Carbon paper was used as the gas diffusion layer for both electrodes. Methanol$-H_2O$ vapor was delivered to the anode using N_2 as a carrier gas. The partial pressure of methanol was varied by independent control of the carrier gas to separate methanol and water spargers. Since water has strong absorption in mid-IR range, D_2O was used for humidification of the reactant gases and the membrane electrode assembly was previously saturated with D_2O prior to insertion into the spectroelectrochemical cell. Humidified D_2 was delivered to the cathode plenum. The cathode was used as a reversible deuterium reference electrode to which all potentials are referenced. The cell was operated at 50 °C.

Results and Discussion

Abnormal Bipolar Bands Due to CO Adsorption on Pt Black Coated with Nafion. The potential dependent spectra of the Pt-black anode surface are shown in Figure 3. The spectra are referenced to the spectrum obtained at 0 V. The bipolar bands appearing at about 2082 cm^{-1} are assigned to linearly bound CO, the primary adsorbed intermediate of methanol oxidation. Our experimental conditions did not give rise to the observance of two and 3-fold bound CO peaks. The upward high-frequency component of the bipolar SNIFTIR bands corresponds to an increase in the IR reflectivity. The positive

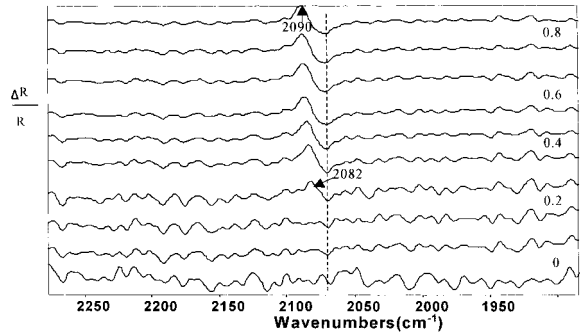

Figure 3. Potential dependent in situ reflection FTIR spectra of the PT anode.

shift of the CO stretching frequency as the potential is increased (vibrational Stark tuning) is well documented.[15−18] the Stark tuning peaks (positive-going bands) indicate an increase in overall reflectivity where there is an increase in absorption by the adsorbed CO. The negative lobes of the bipolar peaks, which are not potential dependent, are a result of a shift of the absorption maximum to higher frequencies from the lower frequency reference absorption. Thus, the reflectivity decreases as the absorption maximum shifts to higher frequency. This results in a bipolar peak that is inverted from what is observed on pure Pt.[19] Inverted bipolar peaks resulting from adsorption of CO, derived from methanol oxidation, on Pt particles deposited on the basal plane of graphite, were reported by Christensen et al..[11] They attributed this phenomenon to a potential-induced migration of chemisorbed CO molecules, from terrace (at reference potential) to edge or kink sites at the sample potential (more positive) because the stretching frequency of CO on terraces is higher (2070 cm^{-1}) than that of CO on edges or kinks (2040 cm^{-1}). Guitiérrez[10] reported inverted bipolar peaks when studying the oxidation of CO on Ir metal deposited on a glassy carbon substrate. However, when polished Ir is used as the substrate, normal bipolar peaks are obtained. They attribute the increase in reflectivity to the properties of the moderately reflective GC substrate. Although still not well understood, the effect is linked to conditions where the supported metal has a thickness of less that the absorption depth (e.g., $d/\lambda \approx 1000$) permitting interaction of the IR radiation with the moderately conducting support material. Adsorbates with high extinction coefficients ($k > 6$) can cause the overall reflectivity to increase when the strong dipole couples with electromagnetic radiation ($\approx$2000 cm^{-1} for adsorbed CO).[20] Lu et al.[12] attributed anomalous bipolar bands to IR emission. They associate the abnormal bipolar bands more to the Pt particle size rather than the substrate material. In addition, the studies of Peter R. Griffiths show that percolation strength, the connections between the Pt island, plays an important role on the band shape by changing the refractive index of system.[32] Our work focuses on CO adsorption and oxidation on fuel cell grade platinum black power supported on the proton conducting polymer electrolyte (Nafion). Figure 3 shows that the bipolar peaks resulting from the Stark shift are above the noise level at 0.3 V. Although a vibrational Stark shift produces bipolar peaks, the CO coverage remains unchanged throughout the potential regime studied. The kinetics of methanol oxidation is sluggish, permitting the oxidized CO to be replenished from the constant feed of methanol to the fuel cell anode plenum. If the coverage were to significantly decrease, the integral of the positive lobe would decrease relative to the negative lobe.

Dependence of DMFC FTIR Spectroscopy on the MeOH/D_2O Ratio. Figure 4 shows the anode potential dependence of

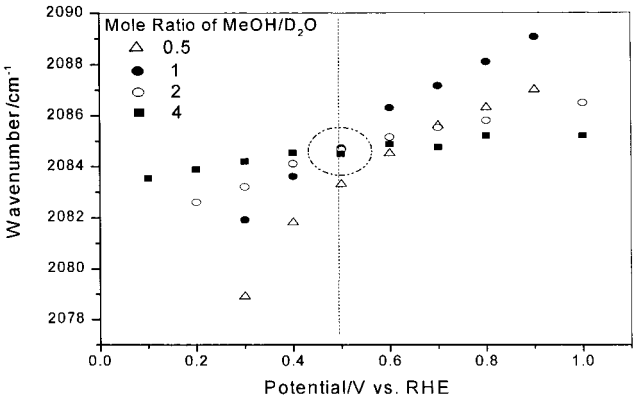

Figure 4. Potential dependence of the linear bonded CO IR peaks vs the methanol:D_2O ratio.

the CO stretching peaks at MeOH/D_2O ratios of 4, 2, 1, and 0.5. It is noteworthy that the band-centers vary positively with potential, due to Stark effect,[16,17] not only in the low-potential region (0.3−0.5 V vs RHE), but also in the higher potential region up to 1 V. As the potential is increased, back-donation of d-band electrons into the antibonding $2\pi^*$ orbitals of the CO_{ads} is reduced, increasing the CO bond order, force constant, and C−O stretching frequency. This has been referred to as the vibrational Stark effect.[16,17] In UHV systems the stretching frequency of CO_{ads} on Pt decreases as the CO is oxidized[21,22] because dipole−dipole coupling is reduced. Kunimatsu et al. observed a Stark tuning region linear up to 0.9 V when CO was adsorbed in the double layer potential region on smooth polycrystalline Pt.[23] He postulated the formation of CO_{ads} islands, with oxidation occurring at the island perimeter. Water is excluded from activation within the islands, thus activation occurs at and beyond the perimeter without disturbing the dipole−dipole environment of CO_{ads} within the islands. Thus, initial variation of the overall coverage does not significantly reduce dipole−dipole coupling. Kunimatsu also studied the spectroscopy and oxidation of CO adsorbed at potentials in the hydrogen region[24] and observed a Stark tuning region with a narrower linear potential window than when the CO is adsorbed at potentials within the double layer, and ascribed this to a more random distribution of CO on the surface, where a diminishing of dipole−dipole coupling would accompany reduction of coverage even at the early stages of oxidation. At 0.5 V the stretching frequency of CO adsorbed in the hydrogen region on smooth electrodes drops off as the CO is oxidatively removed. In Figure 4, although the slopes of STR decrease beyond 0.5 V, the stretching frequencies continue to increase with voltage, even up to 1 V. The coverage of the CO layer formed in an operating direct methanol fuel cell does not change because the CO is replenished by the continuously delivered methanol to the fuel cell anode plenum.

The wavenumber peak trends (Figure 4) appear to rotate around a region located at 0.5 V, as the MeOH/D_2O ratios are varied. Interestingly, if the slope of the 0.5 CH_3OH:D_2O ratio curve did not change at 0.5 V, the four curves would intersect at 2084 cm^{-1}, 0.5 V. This transition point is coincident with the onset of zero order methanol oxidation on Pt anodes consisting of the same catalyst immersed in 0.5−2.0 M methanol in 0.5 M sulfuric acid (Figure 5). Methanol oxidation becomes nonzero order above 0.6 V. As a visual aid, a dotted line is drawn at the transition point position. The Stark tuning slopes[25] decrease at potentials positive of the transition voltage. The Stark tuning rates (STRs) before and after the transition point for the four concentrations studied are tabulated (Table 1).

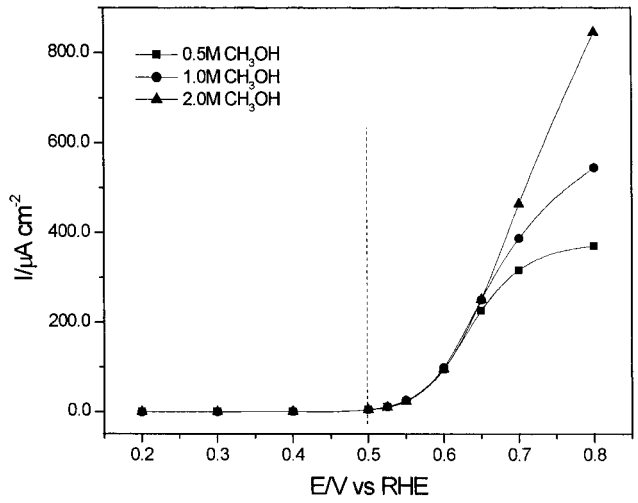

Figure 5. Steady state $I-V$ curves for oxidation of CH_3OH at different concentrations in 0.5 M H_2SO_4 on a Pt black electrode.

TABLE 1: STR versus the MeOH/D_2O Mole Ratio

mole ratio of MeOH/D_2O	0.5	1	2	4
STRs (cm^{-1}/V) < 0.5 V	18.3	14.3	6.54	2.5
STRs (cm^{-1}/V) >0.5 V	8.2	9.2	3.3	1.1

We have measured Stark tuning rates for adsorbed (in the hydrogen region) CO on polished polycrystalline surfaces. The STRs for Pt ranged from 9.8 to 23.8 at coverages from 100% to 68%.[26] The STRs increase as the coverage in decreased. These values should be contrasted with the STRs of the fuel cell catalysts negative of the transition potential (Table 1). The STRs of the Nafion coated fuel cell catalysts are much lower than for the uncoated smooth electrodes.

In summary, we observe that 1) the CO_{ads} STRs decrease as the methanol:D_2O ratio is increased, 2) at potentials positive of the transition voltage, the STRs substantially decrease (especially at the lowest MeOH/D_2O mole ratio and 3) the CO_{ads} IR peaks, blue-shift as the methanol concentration is increased at potentials negative of transition region potential while at potentials positive of the transition voltage, the dependence of the stretching frequency on methanol concentration is weaker and more complex.

In a model describing the interaction between the CO molecule and the metal d states, Nørskov describes the bonding of CO to platinum in two steps.[27,28] In the first step, the $2\pi^*$ and the 5σ MOs are shifted down in energy and broadened due to coupling with the Pt s,p electrons. The renormalized CO orbitals are then mixed with the Pt d-band resulting in the splitting of the $2\pi^*$ MO into antibonding and bonding orbitals. As the mole fraction of methanol is increased, the renormalized CO $2\pi^*$ MO density of states (DOS) are increased. There are more $2\pi^*$ orbitals competing for d-band electrons causing the stretching frequencies to become less sensitive to changes in the extent overlap of the d-band with the renormalized CO orbitals (e.g., At MeOH:D_2O = 0.5, the STR is a factor of 7 larger than when the ratio is 4 at potentials negative of transition region). At the highest methanol/water ratio the STR is anomalously low. At lower methanol concentrations, the overall coverage of CO is lower such that differential changes in the location of the Fermi level affect a greater fraction of the $2\pi^*$ MO density of states integral. Thus, the STR slopes increase as the MeOH:D_2O ratio is decreased.

The change in the slopes, at the transition voltage, can be discussed in light of the work of Ito et al.[29] reporting that the CO adlayer structure changes from (2×2) to $(\sqrt{19} \times \sqrt{19})$ at

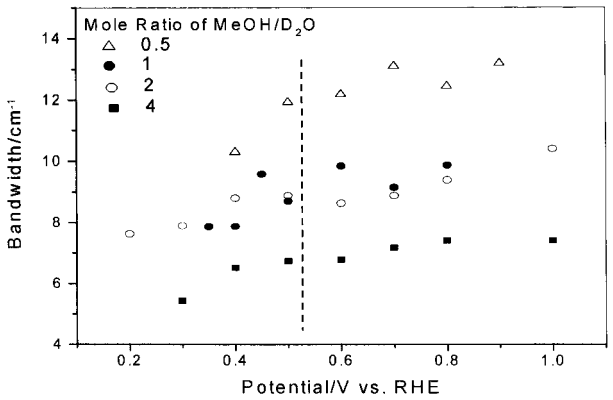

Figure 6. Potential dependence of the CO IR bandwidth vs the methanol:D_2O ratio.

around a potential of 0.4 V. This corresponds to a change in the distance between terminal CO molecules from 5.6 to 12.2 Å resulting in a decrease of dipole−dipole coupling. Also coadsorbed H_2O can donate electron density to the Pt d band, which can in back fill into the CO $2\pi^*$ orbitals resulting in reduced stretching frequencies. Water activation progressively increases with potential after the transition voltage and this could contribute to the reduced slopes.

Methanol oxidation on Pt is zero order below 620 mV.[30] However at potentials negative of 0.5 V, the stretching frequencies still increase with methanol concentration. At higher methanol concentrations the CO coverage per surface atom is increased; there are more $2\pi^*$ MOs competing for d-band electrons resulting in a net decrease in back-donation per adsorbed species. This causes the CO band to blue shift. The higher coverage also increases dipole−dipole coupling, which increases the stretching frequencies as well. Additionally, Vanolli suggests as the coverage is increased, the CO migrates to less active sites resulting in an increase of the stretching frequency.[31] It is clear from these results that the rate-limiting step for methanol oxidation on pure Pt involves water activation, since adsorption of methanol is quite sensitive to methanol partial pressure.

Currently we cannot explain the relationship between the MeOH:D_2O mole ratio and the stretching frequencies at potentials positive of the transition potential (e.g., the highest methanol concentration yields the lowest stretching frequency). The experimental conditions are peculiar to fuel cell operation conditions (i.e., methanol is continuously delivered to the anode). There are a numerous factors that make this potential regime (in an actual fuel cell) more complicated than the conditions of the Kunimatsu study,[23,24] such as the kinetics of CO formation and steady-state oxidation at the electrode surface. Some insights can be gained by examination of the bandwidths as a function of methanol concentration and potential. The bandwidth data of Figure 6 can be viewed as two regimes, negative and positive of the transition voltage (dotted line). It is clear that negative of the transition region the bandwidths are sensitive to changes in the potential. At potentials positive of the transition potential, the bandwidths are independent of potential suggesting constant coverage after 0.5 V. This is consistent with the approximate equality of the integrals of the positive and negative lobes of the bipolar peaks throughout the entire potential range studied

Figure 6 also shows that the bandwidths increase as the methanol concentration is decreased. There are at least two factors affecting peak breadth: (1) electron back-donation increases as the CO coverage is decreased because competition for d-band electrons is reduced (i.e., homogeneous broadening) and (2) band broadening as the methanol concentration is reduced thus increasing the dispersion of adsorption sites. At higher methanol concentrations the CO is more ordered resulting in narrower bandwidths.

Conclusions

Stark tuning rates are studied for the first time on membrane electrode assemblies in operating direct methanol fuel cells as a function of methanol:water ratio. The Stark tuning rates on the Nafion coated fuel cell catalysts are lower than for uncoated polished polycrystalline Pt electrodes. The bipolar peaks resulting from the Stark shifting of the CO absorbance peaks are inverted, indicating an increase in the reflectivity as a result of the infrared absorbing CO. This is the first report of inverted bipolar peaks on CO/Pt supported on an electronically insulating proton conducting polymer. The Stark tuning rates and bandwidth:potential relationships show a discontinuity at 0.5 V, which is coincident with the onset of zero order (with respect to methanol) oxidation on pure Pt. The in situ surface reflectivity studies suggest the necessity of studying catalysts in actual reactor conditions. The Stark tuning data suggest that, as Kunimatsu found for CO adsorbed within double layer potentials, island formation is likely in direct methanol fuel cells where methanol is continuously fed to the fuel cell at and above the double layer region of the unsupported Pt catalyst. At potentials above the transition potential the independence of the bandwidth on the potential also suggests constant coverage even up to 1 V. Work is now in progress to further understand the bandwidth and Stark tuning rate trends at potentials positive and negative of the transition potential and the abnormal infrared absorption effect.

Acknowledgment. The Army Research Office Grants DAAH04-94-G-0055, DAAH04-95-1-0570 and DAAG55-97-1-0198 provided funding.

References and Notes

(1) Gottesfeld, S. Presentation at DOE/ONR Fuel Cell Workshop. Baltimore, MD, October 6−8, 1999.

(2) Reddington, E.; Sapienza, A.; Gurau, B.; Viswanathan, R.; Sarangapani, S.; Smotkin, E. S.; Mallouk, T. E. *Science* **1998**, *280*, 1735.

(3) Gurau, B.; Viswanathan, R.; Liu, R.; Lafrenz, T. J.; Key, K. L.; Smotkin, E. S.; Reddington, E.; Sapienza, A.; Chan, B. C.; Mallouk, T. E.; Sarangapani, S. *J. Phys. Chem. B* **1997,** *102*, 1998.

(4) *Direct Methanol-Air Fuel Cells*; Landgrebe, A. R., Sen, R. K., Wheeler, D. H., Eds.; The Electrochemical Society Proceedings Series, Pennington NJ, 1992; PV 92−14.

(5) Fan, Q.; Pu, C.; Ley, K. L.; Smotkin, E. S. *J. Electrochem. Soc.* **1996**, *143*, L21.

(6) Fan, Q.; Pu, C.; Smotkin, E. S. *J. Electrochem. Soc*. **1996**, *143*, 3053.

(7) Liu, L.; Viswanathan, R.; Liu, R.; Smotkin, E. S. *Electrochem. Solid-State Lett.* **1998**, *3*, 123.

(8) Lu, G. Q.; Sun, Sh. G.; Cai, L. R.; Chen, Sh. P.; Tian, Zh. W. *Langmuir* **2000,** *16*, 778

(9) Christensen, P. A.; Hamnett, A.; Weeks, S. A. J. *J. Electroanal. Chem.* **1988,** *250*,127.

(10) Ortiz, R.; Cuesta, A.; Márquez, O. P.; Márquez, J.; Méndez, J. A.; Gutiérrez, C. J. *Electroanal. Chem.* **1999**, *465*, 234.

(11) Christensen, P. A.; Hamnett, A.; Munk, J.; Troughton, G. L. *J. Electroanal. Chem.* **1994**, *370*, 251.

(12) Lu, G. Q.; Sun, S. G.; Chen, S. P.; Tian, Z. W.; Yang, H.; Xue, K. H. Electrochem. Society Spring Meeting, Los Angeles, Abstr. No. 891.

(13) Pons, S.; Davidson, T.; Bewick, A. *J. Electroanal. Chem.* **1984**, *160*, 63.

(14) Wilson, M. S.; Gottesfeld, S. *J. Appl. Electrochem.* **1992**, *22*, 1.

(15) Lambert, D. L. *J. Chem. Phys.* **1988**, *89* (6),3847.

(16) Villegas, I.; Weaver, M. J. *J. Phys. Chem. B* **1997**, *101*, 5842.

(17) Zou, S. Z.; Weaver, M. J. *J. Phys. Chem.* **1996**, *100*, 4237.

(18) Anderson, A. B.; Kötz, R.; Yeager, E. *Chem. Phys. Lett.* **1981**, *82*, 130.

(19) Iwasita T in Tobias, C. W.and Gerischer, Eds. *Advanced in Electrochemical Science and Engineering*; Wiley-VCH: New York, 1991; Vol. 1, p 127.
(20) McIntyre, J. D. E. In *Advances in Electrochemistry and Electrochemical Engineering*; Delahay, P., Tobias, C. W., Eds.; Wiley: New York, 1973; Vol. 9, p 80, Figure 7.
(21) Shigeishi, R. A.; King, D. A. *Surf. Sci.* **1976**, *58*, 379.
(22) Crossley, A.; King, D. A. *Surf. Sci.* **1977**, *68*, 528.
(23) Kunimatsu, K.; Golden, W. G.; Seki, H.; Philpott, M. R. *Langmuir* **1985**, *1*, 245.
(24) Kunimatsu, K.; Seki, H.; Golden, W. G.; Philpott, M. R. *Langmuir* **1986**, *2*, 464.
(25) Iannsiello, R. S.; Schmidt, V. M.; Stimming, U.; Stumper, J.; Wallau, A. *Electrochim. Acta* **1994,** *39 (11/12)*, 1863.
(26) Liu R.; Iddir, H.; Fan Q.; Hou G.; Bo A.; Smotkin, E. S. *J. Phys. Chem*., in press.
(27) Hammer, B.; Nielsen, O. H.; Nørskov, J. K. *Catal. Lett.* **1997**, *46*, 31.
(28) Hammer, B.; Morikawa, Y.; Nørskov, J. K. *Phys. Rev. Lett.* **1996**, *76* (12), 2141.
(29) Yoshimi, K.; Song, M.; Ito, M. *Surf. Sci.* **1996**, *368*, 389.
(30) Manuscript in preparation.
(31) Vanoli, F.; Heiz, U.; Schneider, W. D. *Chem. Phys. Lett.* **1997**, *277*, 527.
(32) Bjerke, A. E.; Griffiths, P. R.; Theiss, W. *Anal. Chem.* **1999**, *71*, 1967.